High Resolution Millimeter Wave Fabry-Perot Interferometer*

WILLIAM CULSHAW†

Summary—The design and operation of a microwave Fabry-Perot interferometer at wavelengths around 6 mm is described. This uses reflectors which are simple, easy to make, and which are capable of scaling for operation at short wavelengths in the ultramicrowave region. With power reflection coefficients around 0.999, very sharp fringes and Q values around 100,000 were obtained on the interferometer. Effects of diffraction in the interferometer are considered, and wavelength measurements with this particular interferometer indicate that accuracies of 0.04 per cent are obtained without any diffraction correction. Advantages of such an interferometer for ultramicrowaves are that the component parts are large compared with the wavelength, the effects of diffraction decrease with he wavelength, and the problem of maintaining a high Q with a single mode of propagation and a structure of adequate size is made much easier. Such an interferometer forms the cavity resonator for ultramicrowaves. It can thus be used for such conventional purposes as wavelength measurements, wavelength spectral analysis, dielectric constant, and loss measurements, or as the cavity resonator for frequency stabilization, or as the cavity resonator for a millimeter- or submillimeter-wavelength maser.

I. Introduction

BECAUSE of its low loss and high frequency selectivity the resonant cavity forms an almost indispensable component in the fields of microwave techniques and microwave measurements. In general, however, the dimensions of each cavity must be comparable with the wavelength in order to avoid undue trouble from higher order modes; and at shorter wavelengths, say around 1 mm, such cavities would become difficult to make, and difficult to use for many of the conventional purposes and measurements. In addition, for cavities of the same material, shape, and mode of operation, the Q values are proportional to the square root of the resonant wavelength. This leads to a reduced precision in measurements, and to an increased effect of losses in such resonant structures at short wavelengths.

In what may be called the ultramicrowave region of wavelengths,[1] there is thus a definite need for some replacement of the conventional cavity resonator. Since cavities operate on the principle of multiple reflections and interference, it is natural to consider the use of an ultramicrowave form of an optical interferometer to replace the cavity in this region. Thus, the use of a microwave interferometer based on the optical Fabry-Perot interferometer[2] is indicated; the main problem for ultramicrowaves being the design of suitable reflectors with low loss and adequate reflectivity, to give a large number of multiple reflections and hence sharp fringes. This problem has been considered in a previous paper.[3]

The advantages of such an interferometer or cavity resonator for ultramicrowaves are that the reflectors and component parts are large compared with the wavelength. In fact the larger they are the less are the effects of diffraction on the measurements, and instead of becoming more difficult, the problem of maintaining a high Q with a single mode of propagation and a structure of adequate size, becomes easier the smaller the wavelength.

Such an interferometer forms the cavity resonator for ultramicrowaves and can be used for wavelength measurements, wavelength spectral analysis, dielectric constant and loss measurements, and also as a cavity resonator for frequency stabilization, millimeter-wave maser work, or for any other purpose for which microwave resonant cavities are used.

In this paper the results of a pilot investigation on an interferometer employing new reflector designs are presented. The theory of the interferometer, including diffraction effects, is given, and the particular reflector designs used are discussed. This interferometer was operated at a wavelength of 6.28 mm. Values of the reflectivity obtained are given together with the results of wavelength measurements with the interferometer. Fringe sharpness and Q values were also measured, the fringes obtained being extremely sharp in agreement with theory. Some computations on the effects of diffraction for various reflectivities and aperture sizes were also made, the reflectors being assumed infinite in extent.

The results obtained substantiate the great potential use of this interferometer in the ultramicrowave region, and in addition show its use as regards precision measurements of wavelength, and hence the velcotiy of electromagnetic waves.

II. Theory and Diffraction Effects

Fig. 1 shows the symmetrical reflector or multiple interference section of the interferometer. Here r_v is the voltage amplitude reflection coefficient, and t is the amplitude transmission coefficient of a single reflector. Methods for computing these for various reflector designs have been considered in a previous paper.[3] A

* Manuscript received by the PGMTT, September 28, 1959; revised manuscript received, October 26, 1959.

† National Bureau of Standards, Boulder Labs., Boulder, Colo.

[1] I. Kaufman, "The band between microwave and infrared regions," PROC. IRE, vol. 47, pp. 381–396; March, 1959.

[2] F. A. Jenkins and H. E. White, "Fundamentals of Optics," McGraw-Hill Book Co., Inc., New York, N. Y., pp. 269–276; 1950.

[3] W. Culshaw, "Reflectors for a microwave Fabry-Perot interferometer," IRE TRANS. ON MICROWAVE AND THEORY TECHNIQUES, vol. MTT-7, pp. 221–228; April, 1959.

plane wave of amplitude E_0 incident on the reflectors as shown gives rise to waves of amplitudes E_1, E_2, E_3, and E_4 as indicated. The electric and magnetic fields at any point z between the reflectors may then be found by applying boundary conditions, or by the use of multiple reflections,[4] and are given by

$$E = \frac{E_0 t \exp(-jkz)\{1 + r_v \exp[-2jk(d-z)]\}}{1 - r_v^2 \exp(-2jkd)},$$

$$H = \frac{E_0 t \exp(-jkz)\{1 - r_v \exp[-2jk(d-z)]\}}{Z_0[1 - r_v^2 \exp(-2jkd)]}, \quad (1)$$

where $k = 2\pi/\lambda$ for a lossless medium between the reflectors, d is the distance between the reflectors, and $Z_0 = (\mu/\epsilon)^{1/2}$ is the intrinsic impedance for the TEM mode of propagation between them. The impedance at any point z between the reflectors is then

$$Z = E/H. \quad (2)$$

The transmission coefficient t gives the attenuation and phase shift in passing through a reflector, and without loss in generality we may neglect any phase changes which occur on reflection, *i.e.*, put $r_v = r$. The reflector separation d for optimum transmission is then given by

$$2kd = n\pi, \qquad n = 1, 2, 3, \text{ etc.}, \quad (3)$$

where n is the order of interference. The fields between the reflectors for this separation then follow from (1), and the Q value of the reflector system may then be determined from

$$Q = \omega \frac{\text{Energy stored in reflector system}}{\text{Mean dissipation of power in reflector system}}. \quad (4)$$

Since the energy stored is given by $(1/2)\epsilon \int \boldsymbol{E} \cdot {}^*\boldsymbol{E} dv$, and the mean energy dissipated per unit area is given by $(1/2)(1-|r|^2)$ Re $(\boldsymbol{E} \times \boldsymbol{H}^*)$, where the Poynting vector flux is evaluated at the reflector surface, then assuming no loss in the medium between the reflectors, we obtain

$$Q = [n\pi(1 + |r|^2)]/[2(1 - |r|^2)] \quad (5)$$

which is independent of any transmission losses occurring in the reflectors, and depends only on the reflectivity.

Similarly from (1) and (3), maximum and minimum values of the electric field between the reflectors at resonance, *viz.* $2kd = n\pi$, are given by

$$|E|_{\max}^2 = E_0^2 |t|^2 (1 + |r|)^2/(1 - |r|^2)^2; \quad (6)$$

$$|E|_{\min}^2 = E_0^2 |t|^2 (1 - |r|)^2/(1 - |r|^2)^2. \quad (7)$$

If there are no losses in the reflectors, $|t|^2 = 1 - |r|^2$ and (6) and (7) reduce to simpler forms involving only the reflectivity again. Similar equations hold for maximum and minimum values of the magnetic field.

[4] C. G. Montgomery, *et al.*, "Technique of Microwave Measurements," M.I.T. Rad. Lab. Ser., McGraw-Hill Book Co., Inc., New York, N. Y., pp. 561–564; 1957.

To consider the effects of diffraction in the complete interferometer we require the reflection and transmission coefficients r_I and t_I of the interferometer section shown in Fig. 1. These may be deduced from (1) and are given by

$$r_I = \frac{E_1}{E_0} = \frac{r_v[1 + (t^2 - r_v^2)\exp(-2jk_z d)]}{1 - r_v^2 \exp(-2jk_z d)}, \quad (8)$$

$$t_I = \frac{E_4}{E_0} = \frac{t^2 \exp(-jk_z d)}{1 - r_v^2 \exp(-2jk_z d)}, \quad (9)$$

where $k_z = k \cos\theta$ is the propagation constant for a wave incident obliquely on the reflector, θ being the angle between z-axis and the propagation vector k.

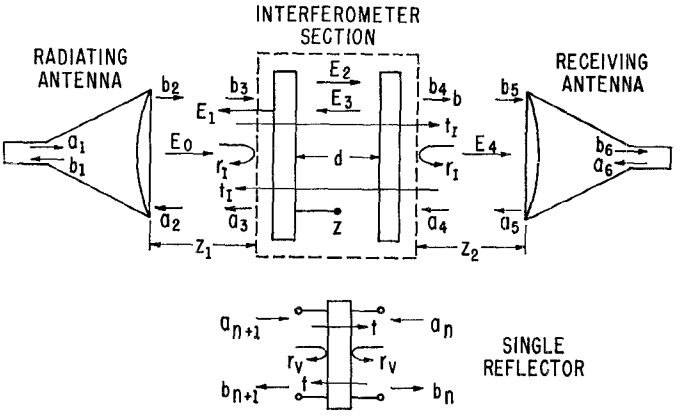

Fig. 1—Diagram for millimeter wave Fabry-Perot interferometer.

The T matrix[5] of the interferometer section shown in Fig. 1, relating the incident and reflected waves, is then given by

$$\begin{bmatrix} b_4 \\ a_4 \end{bmatrix} = \begin{bmatrix} T_{11}^I & T_{12}^I \\ T_{21}^I & T_{22}^I \end{bmatrix} \begin{bmatrix} a_3 \\ b_3 \end{bmatrix} \quad (10)$$

where

$$T_{11}^I = (t_I^2 - r_I^2)/t_I, \qquad T_{12}^I = r_I/t_I = -T_{21}^I,$$

and

$$T_{22}^I = 1/t_1.$$

We may now deduce the reflection and transmission for the complete microwave interferometer, including the radiating and receiving apertures, and the various distances involved. The theory given here is based on the scalar diffraction treatment of the problem instead of on the more precise vector treatment.[6] Some computations of the diffraction correction in a Michelson interferometer[7] showed that the agreement between the sca-

[5] C. G. Montgomery, R. H. Dicke, and E. M. Purcell, "Principles of Microwave Circuits," M.I.T. Rad Lab. Ser., McGraw-Hill Book Co., Inc., New York, N. Y., pp. 150–151; 1948.

[6] D. M. Kerns and E. S. Dayhoff, "Theory of Diffraction in Microwave Interferometry." (Paper to be submitted for publication.)

[7] W. Culshaw, J. M. Richardson, and D. M. Kerns, "Precision Millimeter Wave Interferometry at the U. S. National Bureau of Standards," *Proc. Symp. on Interferometry*, National Physical Lab., Teddington, Eng.; June 9–11, 1959.

lar and vector results is better than one part in 10^8, when the radiating aperture is some 50 wavelengths in extent. It is thus believed that the use of scalar diffraction theory in the Fabry-Perot interferometer is adequate for such aperture sizes, when the reflectors are very large compared with the wavelength, and have a high reflectivity.

The field at any point in front of the radiating or horn apertures used in the interferometer is due to the superposition of waves in the plane-wave spectrum radiated. This is given by

$$g(k_x, k_y) = \frac{1}{2\pi}\int\int E(x, y) \exp [j(k_x x + k_y y)dxdy], \quad (11)$$

where $E(x, y)$ represents the aperture field in phase and amplitude, $g(k_x, k_y)$ is the radiated plane-wave spectrum or spectral density function, and k_x, k_y, k_z are the rectangular components of the propagation vector. Considering now only radiation from the waveguide-horn transducer along a particular direction k, and reception back along this same direction, the reciprocity relation between the radiated and received waves may be found. Representing the scattering matrix of the four terminal thus singled out by $[S]$, and its impedance matrix by $[Z]$, we have[8]

$$[Z] = ([I] - [S])^{-1}([I] + [S])[Z_0] \quad (12)$$

where $[I]$ is the unit matrix, and $[Z_0]$ the diagonal matrix of elements Z_1, the waveguide characteristic impedance, and Z_2, which might be $k_z/\omega\epsilon$ or $\omega\mu/k_z$ depending on the polarization, is the impedance along the z axis of the plane wave considered. Since $Z_{12} = Z_{21}$, *i.e.*, the impedance matrix is symmetric, from (12) we obtain

$$S_{12}Z_2 = S_{21}Z_1. \quad (13)$$

In the scalar approximation the polar angle θ is assumed small and Z_2 is taken as constant, and hence $S_{12} = CS_{21}$ where C is a constant. S_{21} corresponds to the radiated spectral density function $g(k_x, k_y)$, and we may write the scattering matrix of the radiating antenna for the particular direction k considered as

$$\begin{bmatrix} b_1 \\ b_k \end{bmatrix} = \begin{bmatrix} S_{11} & Cg(k_x, k_y) \\ g(k_x, k_y)dk_x dk_y & S_{22} \end{bmatrix} \begin{bmatrix} a_1 \\ a_k \end{bmatrix}. \quad (14)$$

Here a wave of amplitude $g(k_x, k_y)dk_x dk_y$ is radiated, reception for a wave returning along this same direction also being governed by the function $g(k_x, k_y)$. Amplitudes a_1, b_1 and a_k, b_k, respectively, correspond to incident and reflected waves at arbitrary terminals in the waveguide, and at an arbitrary plane $z = 0$, which is taken as the plane of the radiating aperture.

The factor S_{22} represents the portion of the returning plane wave which is scattered by the antenna into a radiation pattern depending on the particular antenna, but which differs greatly from its usual radiation pattern or polar diagram. There will of course be contributions to this scattered radiation from all the other plane waves in the spectrum which is received by the antenna, and this leads to an extremely complicated S_{22} term, and to multiple reflections between any antenna and a reflector. Practically it is necessary to reduce the effect of S_{22} by attention to antenna design, and if necessary to insert additional attenuation between antennas and reflectors to reduce effects of any multiple reflections. In what follows this term is assumed to be small, and it is put into (14) to indicate that these effects can occur.

With this clarification of the S_{22} term, an equivalent T matrix, similar to (10), for the waveguide-radiat ng antenna transducer may be written down appropriately for the cascading of elements in the complete interferometer. Similar matrices may be written for the receiving aperture-waveguide transducer, and for the line lengths z_1, and z_2, shown in Fig. 1, between the antennas and reflectors. From these together with (10), the equation for reflection and transmission through the complete interferometer is obtained in matrix form. As expected the S_{22} term gives rise to multiple reflections and transits in the interferometer. Neglecting these, and with $S_{11} = 0$, *i.e.*, the antennas are matched to the waveguides, the resultant amplitude reflection and transmission coefficients are obtained by integration over the radiated plane-wave spectrum, *viz.*,

$$r_f = C_1\int\int [g(k_x, k_y)]^2 \exp(-j2k_z z_1) r_I dk_x dk_y,$$

$$t_f = C_2\int\int [g(k_x, k_y)]^2 \exp[-jk_z(z_1 + z_2)] t_I dk_x dk_y. \quad (15)$$

Where C_1, C_2 are constants, $g(k_x, k_y)$ is assumed the same for both radiating and receiving apertures and is symmetrical about the normal to the aperture.

The reflectors are considered infinite in extent so that there is no modification, by multiple reflections, of the plane-wave spectrum radiated by the horn aperture, this spectrum then being the one effective in the complete interferometer. The diffraction correction in this case arises from the summation of those plane waves which are passed by the reflector system to give the observed transmission maxima. From (15) we can compute the reflector and transmitted fringe shapes for any radiation pattern $g(k_x, k_y)$, and reflectivity $|r|^2$; deviations from the position of optimum transmission given by (3) then represent the corrections due to diffraction in a wavelength measurement with the interferometer.

Consider the transmission coefficient t_f; the factor t_I due to the reflectors becomes a sharp function for high values of reflectivity, and the reflector system then acts like a plane-wave filter, passing various portions of the radiated spectrum as d is optimized for each plane wave in the spectrum, *i.e.*, when

$$2k_z d = n\pi, \qquad n = 1, 2, 3, \text{ etc.} \quad (16)$$

[8] H. J. Carlin, "An Introduction to the Use of the Scattering Matrix in Network Theory," Microwave Res. Inst., Polytechnic Inst. of Brooklyn, Brooklyn, N. Y., Rept. R-366-54; June 1954.

This is illustrated in Figs. 2 and 3 where the radiation pattern $g(k_x, k_y)$, and the expression $[g(k_x, k_y)]^2 \times |t_I|$ are plotted for a uniformly illuminated slot 24 λ wide, with $n = 50$ and 400, and a reflectivity $|r|^2 = 0.999$. The sharp peaks show how the antenna pattern is scanned by the selective reflector system as the distance d is continuously optimized for various angles θ, since $k_z = k \cos \theta$. In the method of operation considered here we vary d to get the transmitted maximum signal amplitude. Figs. 2 and 3 show how the "fringe" builds up as we scan across the antenna pattern. We have not included phase variations in these considerations, but the results indicate that the position of maximum response will occur when the interferometer is optimized for plane waves close to the axis, *i.e.*, around the $\theta = 0$ position. A similar phenomenon occurs in the optical Fabry-Perot[2] interferometer where a circular fringe system appears, the rings getting sharper as we move out from the center. Since this result would give an accurate measure of the free space wavelength, or propagation constant k, it may be expected that errors due to diffraction will be small for high reflectivities and large reflectors.

This is substantiated by some provisional computations made using (15). Fig. 4 shows the computed fringes obtained for d varying around values corresponding to orders of $n = 160$ and 478, assuming a reflectivity $|r|^2$ of 0.99. The wavelength used in the computations was 6.27817 mm, and the function $g(k_x, k_y)$ used corresponded to that radiated by a 60-cm square apertrue with an H_{10} rectangular waveguide mode field distribution. Wavelengths of 6.278183 mm and 6.271877 mm were obtained from the positions of the computed transmission maxima at the above orders of interference. These results indicate that even at the relatively low values of reflectivity used here, wavelength measurements with very large reflectors are quite accurate. Since a measure of the insertion loss of the interferometer is given for infinite reflectors by the ratio of the areas under the antenna pattern and the curves of $|t_I|\,[g(k_x, k_y)]^2$, it is apparent from Figs. 2 and 3 that the insertion loss in the interferometer will depend on the reflectivity and order of interference used. It will also depend on the width of the radiated angular spectrum. The magnitude of the diffraction correction and the insertion loss can be made smaller with decreasing wavelengths, since apertures and reflectors larger in terms of the wavelength can then be used.

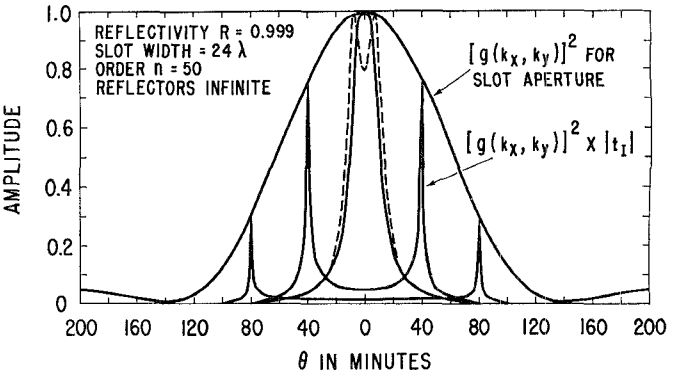

Fig. 2—Scanning of antenna pattern by reflector system, and buildup of fringe in microwave Fabry-Perot interferometer.

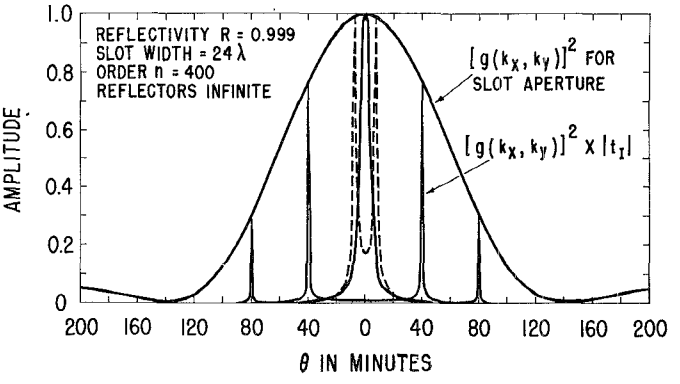

Fig. 3—Scanning of antenna pattern by reflector system and buildup of fringe in microwave Fabry-Perot interferometer.

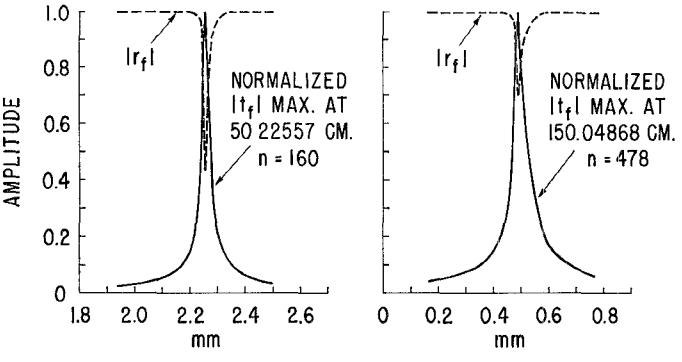

Fig. 4—Computed responses of Fabry-Perot interferometer for infinite reflectors, $|r|^2 = 0.99$, apertures 60 cm square, $\lambda = 6.27817$ mm.

III. Reflector Designs and Reflectivity Measurements

In the microwave region reflectors can be designed using metallic rods, irises, dielectric sheets, etc., suitably positioned on an equivalent transmission line, and for which an equivalent circuit representation may be found. Such methods have been considered previously by the author,[3] where the reflectors consist of capacitive or inductive rod gratings, or perforated hole gratings stacked behind each other. Optimization of the designs and the bandwidth of such structures are also considered. Fig. 5 shows two types of reflectors which have been used on the microwave Fabry-Perot interferometer described here. The rod structure shown is a capacitive type grating, with the electric vector perpendicular to the rods. A number of such gratings are stacked behind each other at the spacing for optimum reflectivity. The rods were made from steel "drill-rod," the diameter of which is held to fairly close tolerance, and which is fairly straight. Different numbers of layers or gratings could be used and the change in reflectivity studied. In this design the rods were $\frac{1}{16}$ inch in diameter, the spacing between the rods in a grating was

0.103 inch, the spacing between gratings was $\lambda/2$, the apertures were 7.5 inches square, and the wavelength was 6.28 mm.

The other reflector shown in Fig. 5 consists of a single brass plate $\frac{1}{32}$ inch thick with holes $\frac{1}{16}$ inch in diameter. The holes were drilled in it at a $\frac{1}{8}$-inch spacing. A number of these could be stacked behind each other, but calculations show that the reflectivity from one such sheet is quite high. This is found by using the approximate rule for the transmission coefficient of a small hole in a thick plate,[9] which gives a value of $|r|^2=0.9993$ for the single perforated brass plate.

In Fig. 6, which shows the complete interferometer, the reflectivity was measured by observing the transmission coefficients of the reflectors. Two horn-lens apertures were used as shown, and the insertion loss due to placing a carefully aligned reflector between them was measured. There were multiple reflection effects between the reflector and the horn antennas, and a mean value of insertion loss was used. The measured reflectivity of the plate was 0.9993; this high value clearly indicating the potentialities of this structure for obtaining sharp fringes on the interferometer. Table I shows the reflectivity from various layers of rods in the capacitive grating; the agreement with calculated values is quite reasonable. These extremely high reflectivities clearly indicate the advantages of a microwave Fabry-Perot interferometer, as regards fringe sharpness, over its optical counterpart.

IV. The Interferometer and Results

Fig. 6 shows a photograph of the interferometer with the 6-inch-square radiating horn-lens aperture on the left and a similar receiving horn on the right. Radiation at a wavelength around 6.278 mm is obtained by multiplying up from a quartz-crystal-controlled oscillator at 5.525 mc, which gives a source stable in frequency to a few parts in 10^8, and with a reasonably steady power output of 1 mw or so at 47,736 mc. By adjustment of a small capacitance in the 5.525-mc oscillator circuit, the frequency can be changed over a range of 12 mc around 47,736 mc. The radiation is then incident on the reflector system, the reflectors being supported on the large aluminum blocks which contain ball bushings and which slide on the supporting steel rods shown. Superheterodyne detection is used at the receiver, a QK294 klystron, frequency stabilized to a high Q resonant cavity after the method of Pound[10] and acting as a local oscillator at 47,706 mc. This is followed by an IF amplifier, a dc amplifier, and the Esterline-Angus recorder. One of the reflectors can be moved slowly by a lead screw and motor drive, and the fringes can be recorded. In addition, there are micrometers for accurate setting of the reflector, and also provision for measuring the change in reflector separation by length gauges, and hence for determining the number of fringes in a given displacement of the moveable reflector.

To set up the interferometer, the horn apertures are aligned along the axis of the reflector carriage, and adjusted for optimum signal without the reflectors. The reflectors are then inserted in their mounts, which have various screw adjustments for setting the reflector surfaces parallel and perpendicular to the axis. Some adjustments of these are made until a transmitted fringe is seen when moving the reflectors apart. These reflector adjustments are rather critical at the high reflectivities involved here, and they are continued until the cleanest and sharpest possible fringe is obtained. Maladjustment of the reflectors can lead to various fringe shapes; each

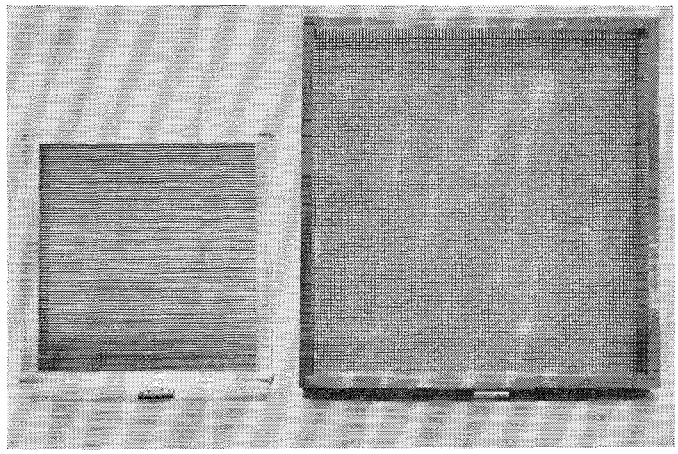

Fig. 5—Capacitive rod gratings and perforated plate reflectors for millimeter wave Fabry-Perot interferometer.

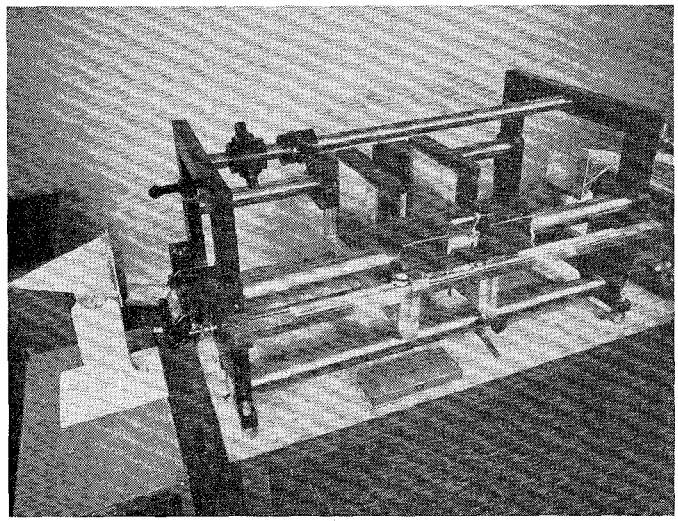

Fig. 6—Millimeter wave Fabry-Perot interferometer.

TABLE I

Calculated and Measured Values of Reflectivity from a Number n of Stacked Capacitive Rod Gratings

n	1	2	3	4	5
$\lvert r_n\rvert^2$ measured	0.4635	0.9000	0.98415	0.999	0.99976
$\lvert r_n\rvert^2$ calculated	0.4854	0.8796	0.97699	0.99683	0.99925

[9] C. G. Montgomery, R. H. Dicke, and E. M. Purcell, *op. cit.*, p. 201.

[10] R. V. Pound, "Electronic frequency stabilization of microwave oscillators," *Rev. Sci. Inst.*, vol. 17, pp. 490–505; November, 1946.

fringe may consist of two separate sharp maxima, or there may be a number of smaller fringes associated with the main maximum. This reflector adjustment is critical and tedious, and the use of optical collimation methods would probably lead to a more satisfactory procedure.

Fig. 7 shows the increase in sharpness of the fringes for 1, 2, and 3 layers of the capacitive rod gratings discussed in Section III. In addition to the sharpening of the fringes, the signal at the minimum between the fringes decreases towards the noise level. Further layers were added but no additional sharpening of the fringes was observed. This is without doubt due to the relatively small reflector area used here, *viz.* 7.5 inches square, since the multiple reflections between the finite reflectors will modify the angular spectrum of radiation between them, and this becomes the dominant effect at relatively high reflectivities. For large reflectors the fringe sharpness for 4 layers would increase over that obtained for 3 layers.

Fig. 8 shows the very sharp transmitted fringes obtained with the 12-inch-square perforated plate reflector at a reflector-separation of 7 inches. The spacing between the fringes corresponds to $\lambda/2$ or 3.14 mm, and the complete fringe occupies a length of about 5×10^{-4} inches. Similar fringes were obtained for a reflector-separation of 30 inches, except that the fringes became somewhat wider. This effect is mainly due to the finite size of reflectors used, but it also depends on the radiating aperture size used, and could be reduced by the use of larger (in terms of the wavelength) apertures and reflectors. Even so, these fringes are the sharpest ever obtained on a Fabry-Perot interferometer, and the importance and use of this interferometer as the cavity resonator for ultramicrowaves is clearly indicated.

Another measure of fringe sharpness may be defined by

$$Q_d = \lambda/2\Delta d, \tag{17}$$

where Δd is the displacement from the maximum- to the half-intensity points on the fringe. Since [3] $Q_d = nQ/2$ it follows from (5) that

$$Q_d = \pi(1 + |r|^2)/(1 - |r^2) \tag{18}$$

and for $|r|^2 = 0.999$ this gives $Q_d = 628^0$. With the perforated plate reflectors Q_d, values of 2000 and 530 have been measured at reflector-separations of 25 cm and 75 cm, respectively. The theoretical value of Q_d given by (5) assumes a single plane wave in the interferometer, whereas the antenna radiates a whole spectrum of these of a width dependent on its dimensions and field distribution. Apertures 6 inches square were used here, the beamwidth or plane-wave spectrum extending at least some 2° either side of the central maximum. In addition the effects of the finite reflector size, particularly at the larger reflector-separations, and the scanning of the antenna pattern at the larger reflector-separations, all contribute to an increase in the measured fringe width.

Fig. 9 shows the increase in fringe width with reflector separation for the 6-inch-square apertures and 12-inch-square reflectors. In addition there is a falling off in the intensity of the fringes as the reflector-separation is increased. At a reflector spacing of 6 inches, the insertion loss of the reflector system is around 15 db. This is due to the selectivity of the reflector system, as is evident from Figs. 2 and 3. For a larger order of interference the selectivity increases, assuming infinite reflec-

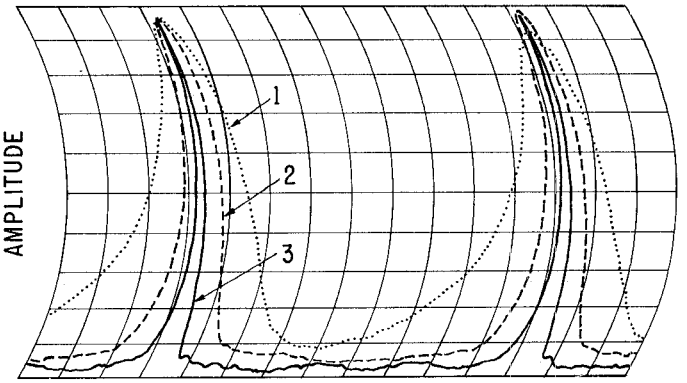

Fig. 7—Fringes for 1, 2, and 3 layers of capacitive rod gratings. $\lambda = 6.28$ mm, reflectors 7.5 inches square and 10 inches apart.

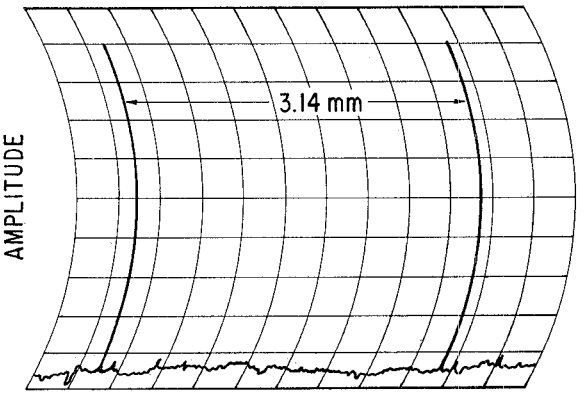

Fig. 8—Fringes on interferometer with perforated sheet reflectors. Reflectors 12 inches square, 7 inches apart, $\lambda = 6.28$ mm.

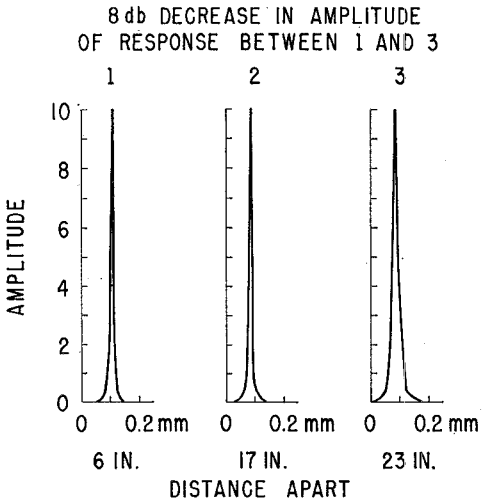

Fig. 9—Showing increasing fringe width with reflector separation. 12-inches-square perforated sheet reflectors.

tors, and the insertion loss will increase. There will also be, in this case, effects due to the finite reflector size used, and in the present experiment an increase in insertion loss of some 8 db occurs when the reflector separation increases from 6 inches to 23 inches.

Frequency selectivity measurements were made on the 12-inch-square perforated sheet-reflectors by changing the frequency of the quartz-crystal oscillator in the frequency multiplier chain. Results were obtained for reflector separations of 6 inches and 17 inches, and gave values of 87,000 and 116,000, respectively, for Q. The frequency selectivity is thus extremely high for the wavelength used, *viz.* 6.28 mm, and could probably be made higher. Similar results can be obtained at still shorter wavelengths and the interferometer has great potential use for measurements and devices in the ultramicrowave region.

Variations in the width of the same fringe for various reflector dimensions are shown in Fig. 10 for a reflector spacing of 25 cm. The increase in fringe width for the smaller reflectors is evident, and there is also a reduction in the intensity of the fringes with the smaller reflectors. Similar results were obtained at reflector spacings of 75 cm, the fringes being some 4 or 5 times wider than those shown in Fig. 10. At a 25-cm spacing the difference between fringes for 12-inch- and 10-inch-square reflectors is not very great. Here the antenna pattern is beginning to be the dominant thing as regards fringe width. At the larger spacing the difference between 12-inch- and 10-inch-square reflectors is more pronounced, and the use of larger reflectors would reduce the fringe width. As already indicated the fringes are quite sharp, since one large division on the abscissa of the chart corresponds to 1.75×10^{-3} inches.

The wavelength of the radiation was measured on the interferometer by starting with an initial reflector separation and counting the number of fringes in a given displacement. For this initial work the displacement was measured with Pratt & Whitney end gauges mounted in the V groove shown in Fig. 6; the results are shown in Table II. For these measurements, the distance between the radiating and receiving horns was 72 inches, and the distance to the first reflector from the radiator was 26.5 inches; this reflector was fixed in position. Taking the velocity of light as $c=299{,}792.5$ km/second,[11] and the known frequency of 47,736 mc, the following values of wavelength are obtained. For n, the refractive index of the air surrounding the interferometer, equal to 1.0003, $\lambda_{air}=6.27835$ mm, and for $n=1.0002$, $\lambda_{air}=6.27896$. The refractive index n was not measured, but is expected to be within the above range. For the present purposes of comparison it is sufficient to use the mean values of Table II, and the mean of the calculated wavelength in air; then the discrepancy amounts to 0.04 per cent, the measured values being too high. For precision measurements a diffraction correction must be applied to the measured values based on (15), and the effect of a finite reflector size on the measurements investigated further. The displacements would also have to be measured more accurately than in this case. Nevertheless, the present agreement between measured and computed wavelengths is good enough for many purposes, even without any diffraction or other corrections, the error being around 0.04 per cent for this particular interferometer. This accuracy is better than that of most commercial resonant cavity wavemeters at this frequency, and the superiority of the interferometer would be much more evident at shorter wavelengths.

[11] K. D. Froome, "A new determination of the free-space velocity of electromagnetic waves," *Proc. Roy. Soc. (London) A*, vol. 247, pp. 109–122; September, 1958.

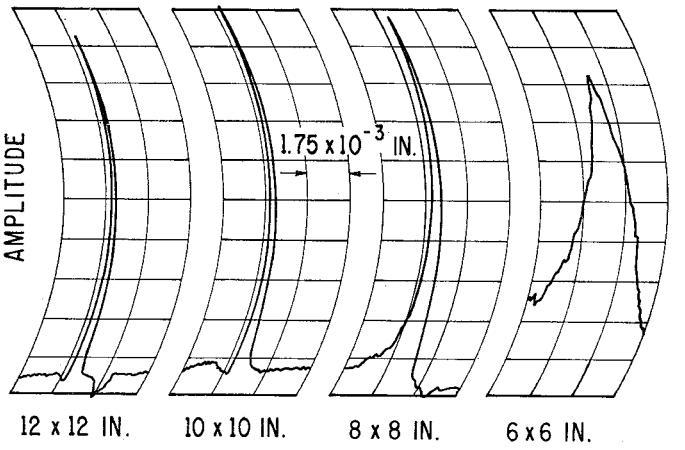

Fig. 10—Variation in fringe shape with reflector size. Perforated sheet reflector, dimensions shown. Spacing $d=25$ cm.

TABLE II
RESULTS OF WAVELENGTH MEASUREMENTS WITH THE MICROWAVE FABRY-PEROT INTERFEROMETER

Initial reflector separation, in inches	Number of fringes	Reflector size, in inches	Measured wavelength, in millimeters
7	97	12×12	6.28102
7	97	10×10	6.28108
7	97	8×8	6.28108
7	146	12×12	6.28142
7	146	10×10	6.28146
20	97	12×12	6.28138
23	146	12×12	6.28100
23	146	10×10	6.28118

V. Conclusions

The results obtained here on the microwave Fabry-Perot interferometer are very significant, and indicate its great potential use at millimeter and submillimeter wavelengths. The microwave reflector designs used here at 6-mm wavelengths give the required high values of reflectivity, are relatively simple and easy to make, and thus permit the use of reasonable scaling factors for operation with ultramicrowaves. A high value of wavelength resolution has been obtained with the present interferometer, and this would be useful in the wave-

length analysis of millimeter wavelength sources too high in frequency to be measured conventionally.

Operating in the TEM mode the interferometer represents the ideal form of cavity resonator, permitting the use of relatively large structures at very small wavelengths with complete freedom from troubles due to higher order modes. The Q values obtained here are higher than can readily be attained by a conventional cavity resonator at these frequencies, and the indications are that still higher Q values can be obtained for apertures and reflectors larger in terms of the wavelength. As the cavity resonator for ultramicrowaves, the use of the interferometer for dielectric constant and loss measurements on both solids and gases is clearly indicated, and in the ultramicrowave region of the spectrum such a method becomes most advantagoues. Its use in all other microwave devices employing a cavity is also possible, and in particular it would appear that the interferometer can be used with facility as the cavity resonator for masers designed to operate at millimeter and submillimeter wavelengths.

Aperture and reflector dimensions of 24 λ and 50 λ, respectively, in extent were used here, and the insertion loss at optimum transmission is around 15 db. Consequently, the reflected power is quite high so that the fringes are best observed in transmission. For smaller wavelengths the problem of adequate aperture and reflector dimensions in terms of the wavelength becomes easier, and interferometers for specific purposes such as maser cavities become easier to accommodate and use with the associated apparatus. Also with apertures and reflectors which are large in terms of the wavelength, the problem of the diffraction correction becomes less severe and important, and the ease with which the interferometer can be used for precision measurements such as the velocity of light, and as a microwave standard of length, will improve with the use of shorter wavelengths.

VI. Acknowledgment

The author would like to thank Dr. D. M. Kerns and Dr. J. M. Richardson for valuable discussions on the work; Dr. P. F. Wacker and W. T. Grandy Jr. for the numerical analysis and programming required in computing values of the diffraction integrals; M. G. Humpal for his careful work in the construction of the interferometer; and H. E. Bussey for his helpful comments on the paper.

Boundary Conditions and Ohmic Losses in Conducting Wedges*

ROBIN M. CHISHOLM†

Summary—**The present work is concerned with the boundary conditions required to calculate the ohmic losses occurring in metallic wedges under the influence of electromagnetic waves which are sinusoidal in time. The validity of the surface impedance condition used in calculating waveguide wall losses is examined carefully, and a "modified" surface impedance condition, which can be applied to wedge problems in which the perfectly conducting solution is known, is developed. A simple waveguide having a circular cross section, a sector of which is occupied by a metal wedge, is used as an example. The tangential magnetic field variations along the surface of the wedge are shown graphically, demonstrating, near the tip of the wedge, a large deviation from the tangential magnetic field of the perfectly conducting solution.**

* Manuscript received by the PGMTT, July 20, 1959; revised manuscript received November 5, 1959. This work was supported by a grant extended to the Dept. of Electrical Engrg., University of Toronto, Toronto, Can., by the Defence Res. Board of Canada under Extramural Res. Grant DRB 5540-02.

† Dept. of Electrical Engrg., Queen's University, Kingston, Ontario, Canada.

I. Introduction

THE heat losses within any conducting object caused by the presence of an electromagnetic field, can be calculated by calculating the average flow of power into the object as a result of the tangential fields on its surface. The boundary conditions which must be imposed on the surface of a metallic wedge in order to calculate this power flow must be considered very carefully. The standard surface impedance condition used in the calculation of waveguide wall losses relates the tangential electric field at a conducting boundary to the known tangential magnetic field which would exist at the boundary if it were perfectly conducting. This condition, when applied to wedge problems, often leads to fields which do not satisfy the Meixner edge condition [1] and to infinite power losses in the region of the tip.